JOURNAL OF MAGNETIC RESONANCE IMAGING 31:101–109 (2010)

Original Research

Magnetic Resonance Imaging in Real Time: Advances Using Radial FLASH

Shuo Zhang, MSc, Kai Tobias Block, PhD, and Jens Frahm, PhD*

Purpose: To develop technical advances for real-time magnetic resonance imaging (MRI) that allow for improved image quality and high frame rates.

Materials and Methods: The approach is based on a combination of fast low-angle shot (FLASH) MRI sequences with radial data sampling and view sharing of successive acquisitions. Gridding reconstructions provide images free from streaking or motion artifacts and with a flexible trade-off between spatial and temporal resolution. Immediate image reconstruction and online display is accomplished with the use of an unmodified 3 T MRI system. For receive coils with a large number of elements this process is supported by a user-selectable channel compression that is based on a principal component analysis and performed during initial preparation scans.

Results: In preliminary applications to healthy volunteers, real-time radial FLASH MRI visualized continuous movements of the temporomandibular joint during voluntary opening and closing of the mouth at high spatial resolution (0.75 mm in-plane) and monitored cardiac functions at high temporal resolution (20 images per second) during free breathing and without synchronization to the electrocardiogram.

Conclusion: Real-time radial FLASH MRI emerges as a simple and versatile tool for a large range of clinical applications.

Key Words: real-time MRI; cardiovascular MRI; temporomandibular joint; radial MRI
J. Magn. Reson. Imaging 2010; 31:101–109.

NONINVASIVE IMAGING of physiological processes in humans without the need for breath-holding or synchronization with the electrocardiogram is a long-standing desire since the advent of MRI (1). In this context, "real-time MRI" refers to the acquisition, reconstruction, and display of magnetic resonance images without any unnecessary or even detectable delay. This definition describes the ultimate requirements for monitoring therapeutic interventions under MRI guidance and deliberately ignores offline reconstruction strategies with more advanced but slow mathematical algorithms. The generic solution advanced here combines the fast low-angle shot (FLASH) technique as a physical principle for rapid and continuous MRI (2) with radial sampling of the spatial information as originally proposed by Lauterbur in his seminal paper on MRI (1). Although radial FLASH MRI was conceived as early as 1985 (Frahm et al, German Patent P 3504734.8, 12 February 1985), experimental realizations were hampered by technical inaccuracies of the early MRI systems, which inescapably led to a predominance of Cartesian sampling schemes.

Cartesian MRI covers the data space in a rectilinear manner, which not only offers a direct and fast image reconstruction by fast Fourier transformation (FFT), but also partially compensates for off-resonance effects and technical inadequacies in gradient performance. On the other hand, Cartesian attempts at dynamic imaging (2,3) suffer from two major disadvantages that limit their usefulness for real-time MRI: 1) because motion induces phase errors into the MRI signal, the use of a phase-encoding magnetic field gradient for spatial encoding results in inconsistencies for moving objects that translate into "ghosting" artifacts in the reconstructed image, and 2) in a rectilinear grid, the individual lines are not equivalent, as they encode either low or high spatial frequencies (in the direction of the phase-encoding gradient). This has unfortunate consequences for any undersampling strategy and, even more important, affects the update properties of Cartesian images when studying moving objects: serial images show the object in its new position only after updating the central low spatial frequencies, which causes the object to remain in its former position for a number of images before "jumping" to the new position in a respective movie sequence. While this may perhaps be tolerable as long as the update time for the central views is still adequate for portraying the phenomenon under investigation, it does not meet the conditions required for high-speed real-time applications as in cardiac MRI. Noteworthy, the same general arguments hold true for Cartesian

Additional Supporting Information may be found in the online version of this article.

Biomedizinische NMR Forschungs GmbH am Max-Planck-Institut für biophysikalische Chemie, Göttingen, Germany.

*Address reprint requests to: J.F., Biomedizinische NMR Forschungs GmbH am Max-Planck-Institut für biophysikalische Chemie, 37070 Göttingen, Germany. E-mail: jfrahm@gwdg.de

Received March 24, 2009; Accepted September 28, 2009.
DOI 10.1002/jmri.21987
Published online in Wiley InterScience (www.interscience.wiley.com).

schemes that are accelerated by parallel imaging methods.

Trials to overcome some of these problems by even faster imaging techniques with echo-planar or spiral samplings (4–7) add new problems due to their use of gradient echoes with prolonged readout times that are sensitive to resonance offset effects. Apart from the fact that respective sequences exhibit a limited useful echo train length, which restricts the spatial resolution, they require the suppression of fat signals and introduce a pronounced sensitivity to magnetic field inhomogeneities that in many regions of the body are caused by the presence of air-filled cavities next to the tissues under investigation. Further magnetic field inhomogeneities may be due to biopsy needles or other surgical instruments, which compromises the use of single-shot echo-planar or spiral techniques for real-time interventional MRI.

All these difficulties and limitations vanish when replacing Cartesian by radial data sampling: the approach yields a set of rotated lines in *k*-space ("spokes") that are of equal importance for image reconstruction, although not identical in their information content. Whereas Cartesian lines in *k*-space differ significantly in representing either high or low spatial frequencies in the phase-encoding dimension, radial spokes always cross the center of *k*-space. This steady update of both low and high spatial frequencies as part of each spoke considerably reduces the occurrence of discontinuities in sliding window reconstructions of moving objects. Moreover, a reduction of the total number of spokes per image does not significantly deteriorate the spatial resolution of the resulting image, but primarily affects its signal-to-noise ratio (SNR). This robustness of radial acquisitions to moderate undersampling is well established (for example, see Refs. 8,9). Even in extreme cases with a very low number of spokes the image is not affected by a loss of object detail but an increasing amount of incoherent streaking artifacts, which usually remain distinguishable from the object under investigation (10).

With respect to real-time applications, radial MRI with the now commonly employed gridding reconstruction method poses no general problem for the computers of commercial MRI systems. Similar arguments hold true for the necessary correction of timing inaccuracies that are observed for the radial sampling gradients (11). Thus, in contrast to many earlier attempts at real-time MRI, which used retrospective or even offline reconstructions of rapid continuous acquisitions or relied on high-performance computers bypassing the existing MRI system, the development presented here allows for a true real-time acquisition, reconstruction, and immediate online display without any modifications of the standard MRI hardware.

MATERIALS AND METHODS

Real-Time Radial FLASH MRI

As shown in Fig. 1a,b, the proposed method comprises both a spoiled and refocused FLASH version for achieving T1 or T1/T2 contrast, respectively. It further employs a view-sharing technique, which allows for reconstruction update periods shorter than the acquisition time of a full dataset. This strategy has previously been developed as MRI fluoroscopy (3,12). The actual implementation employed an interleaved multiturn scheme for radial sampling as outlined in Fig. 1c. The view-sharing for sliding window reconstructions was performed after completion of each turn of the radial acquisition.

Previous attempts to use FLASH MRI in conjunction with radial sampling have exclusively been based on refocused (13–15) or even fully balanced (16–21) gradient-echo sequences with high flip angles in the range of 45–80° for radiofrequency (RF) excitation. These conditions are not necessarily optimal for several reasons: 1) real-time images with T1 contrast cannot be obtained; 2) refocusing magnetic field gradients prolong the minimum repetition time and therefore increase the image acquisition time; 3) the T1/T2 contrast of a refocused or balanced gradient-echo sequence is not always desirable, as it emphasizes tissues (body fluids) with long T2 relaxation times; 4) the use of high flip angles is not even necessary for obtaining T1/T2 contrast when the repetition times TR are as short as 2–3 msec; 5) high flip angles bear the risk of damaging the excited slice profile, which may compromise the achievable image quality; and 6) markedly increase the RF power absorbed by the tissue. This latter feature may become a serious limitation for interventional MRI as one of the most promising real-time applications. In contrast, the real-time MRI sequences proposed here use flip angles in the range of only 5–20°.

It should be noted that the actual implementation of radial FLASH MRI sequences also allows for the use of fully balanced gradient schemes (at no cost in TR compared to refocused versions). However, preliminary testing in various body parts did not result in robust image quality—at least not for a field strength of 3 T. The underlying reason is the extreme sensitivity of fully balanced MRI sequences to resonance offset effects. This seems to pose a general problem for dynamic studies, for example, of moving joints, because it is impossible to guarantee the best magnetic field homogeneity for all positions of a moving joint. As evidenced by experimental observations, movements through areas with slightly different magnetic field strengths cause spatially variable "banding" artifacts in serial real-time images. Fully balanced versions were therefore discarded for the purposes of this study.

Image Reconstruction

Image reconstructions were based on a conventional gridding algorithm (22) comprising a density compensation, a convolution with a Kaiser–Bessel kernel, and an interpolation to a regular grid (23). This was followed by an inverse FFT and a roll-off correction compensating for the imperfect interpolation in *k*-space. For the Kaiser–Bessel kernel a width of $L = 3$ (in units of m^{-1} for a normalized field of view [FOV] of 1 m) and a shape parameter $\alpha = 4.2054$ were chosen, as

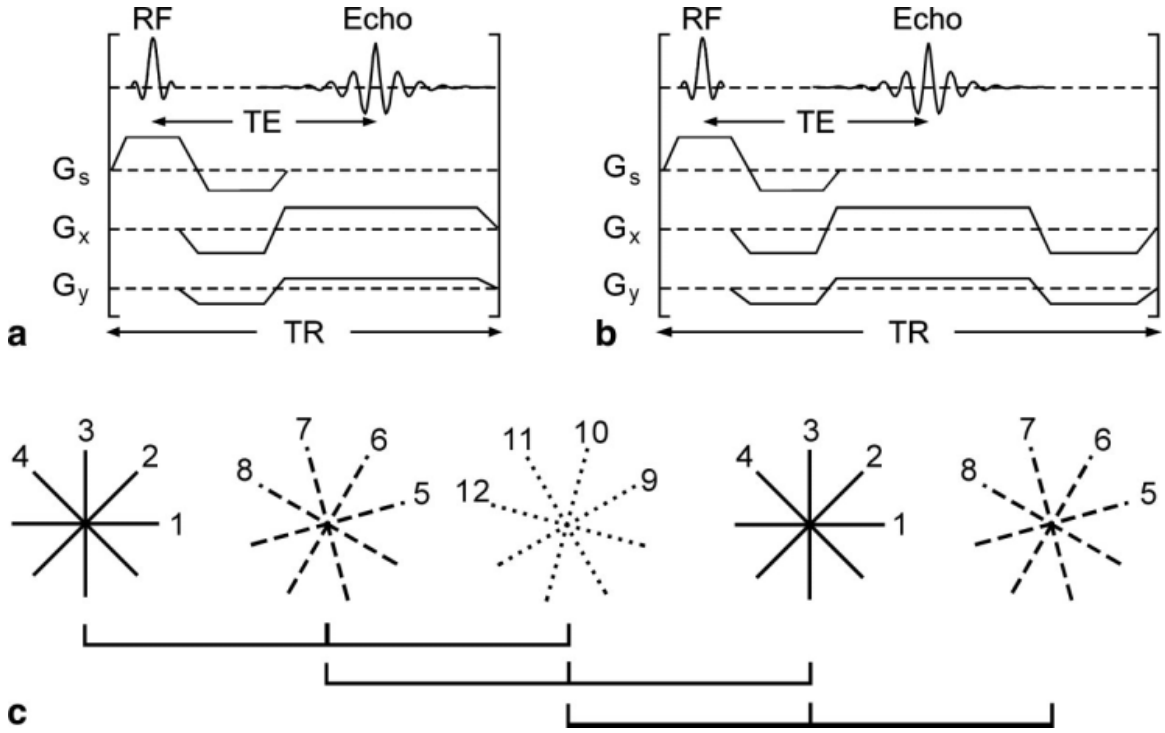

Figure 1. Real-time MRI. **a:** Fast low-angle shot (FLASH) gradient-echo sequence with radial sampling for T1-weighted imaging: RF, radiofrequency excitation pulse; Echo, gradient echo; TE, echo time; TR, repetition time; G_s, slice-selective gradient; G_x and G_y, radial sampling gradients. **b:** Alternative version with refocused encoding gradients for imaging with T1/T2 contrast. **c:** Radial sampling employs multiple interleaves covering the data space in a corresponding number of 360° turns. The example refers to an image with 12 spokes and three interleaves. View-sharing of partial datasets from successive acquisitions, here for each turn, allows for sliding window reconstructions with image update times shorter than a complete acquisition.

previously suggested (24). To prevent aliasing effects from object structures outside the selected FOV, data acquisitions employed a readout oversampling by a factor of two at no extra cost, that is, without compromising TR or SNR. After gridding the correspondingly larger image was cropped to the desired FOV. Noteworthy, the ability to simultaneously perform readout oversampling in both image dimensions represents another fundamental advantage of radial sampling, which is perfectly suited for real-time applications.

Receive Channel Compression

The increasing use of receiver coils with very high numbers of independent elements considerably increases the computational load for image reconstruction. For example, for the MRI system used here and a 32-element receive coil such conditions caused a noticeable delay of about 10 seconds between the end of a 1-minute real-time acquisition and the online display of the last reconstructed image. The problem is solved by the implementation of a software-based receive channel compression (25,26). Accordingly, incoming signals from the individual coil elements are combined into a small set of compressed channels. Because this combination is much faster than a full processing of the signals from all receive channels, the images are reconstructed and displayed with negligible latency, as evident from the synchrony with the acoustic gradient sounds.

Briefly, channel compression is achieved by generating linear combinations of the incoming signals, where the complex-valued combination weights vary for every input and output channel. These weights are estimated by a principal component analysis (PCA) using data from one of the preparation scans employed for steady-state equilibration and kept fixed afterwards. For the PCA, a covariance matrix is constructed by calculating the covariances of the received signals among all combinations of channels, here yielding a 32×32 matrix that describes the inter-channel correlations. By conducting a singular value decomposition of the covariance matrix, a transformation matrix is obtained that contains the desired weights for combining the receive channels into uncorrelated eigenmodes. The weights are directly sorted in descending order according to the energy content of the corresponding eigenmodes. Because most coil arrays carry a certain degree of redundancy due to spatial overlap of the sensitivities from individual coil elements, the higher eigenmodes contain only marginal image information. Therefore, a compression without a recognizable loss in image quality may be achieved by restricting the combination to only a limited number of channels. In general, the degree of usable compression depends on the object under investigation and, more important, on the geometry of the

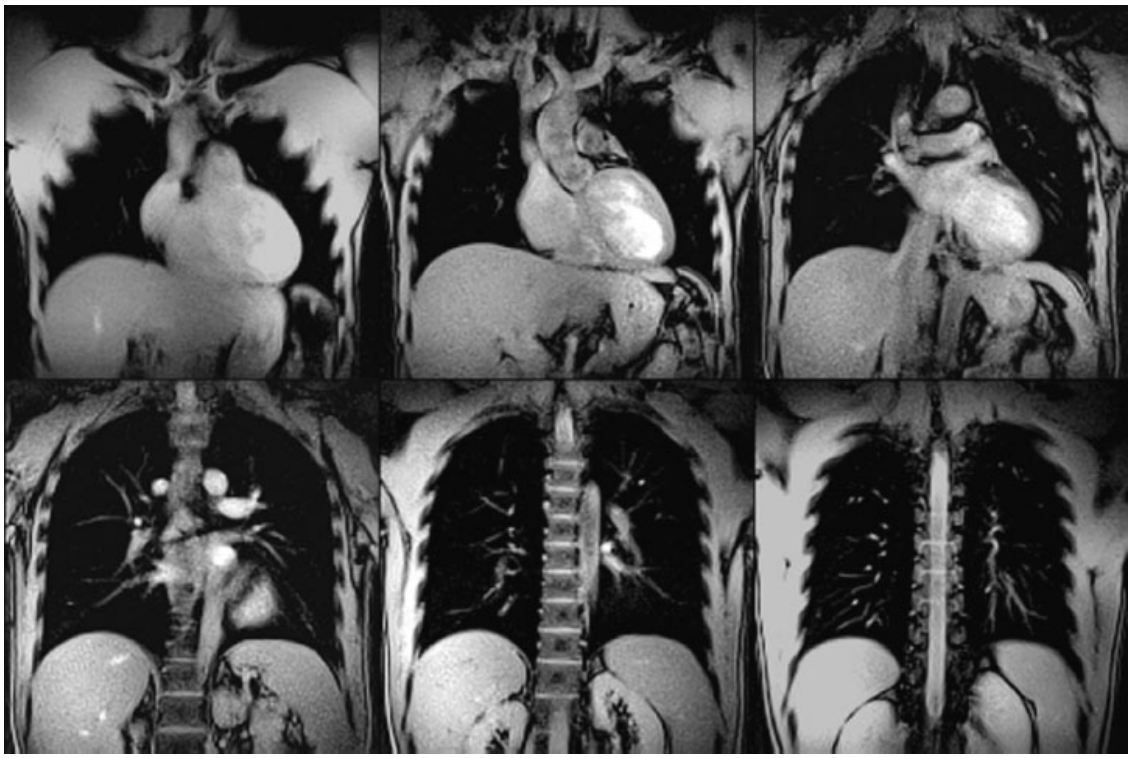

Figure 2. Motion robustness of spoiled radial FLASH images of the heart (500 msec each) from a sequential multislice acquisition (contiguous coronal views, top left to bottom right) with an in-plane resolution of 2 mm and a slice thickness of 8 mm (TR/TE = 2.02/1.30 msec, flip angle 8°, FOV 320 mm, base resolution 160, 245 spokes).

coil array. The channel compression method was therefore integrated into the system's software structure and the feature provided as a user-selectable tool for radial FLASH MRI sequences.

Human Studies

During the course of this work a large number of young healthy adults with no known abnormality participated in real-time examinations including experimental optimizations as well as preliminary applications to different procedures (eg, speaking, swallowing) and organ systems (eg, joints, abdomen, heart). Here, selected results from a limited number of volunteer studies serve to demonstrate the method, whereas serious clinical trials are beyond the scope of this work. All subjects gave written informed consent before each MRI examination.

Real-time MRI was conducted at 3 T (Tim Trio, Siemens Healthcare, Erlangen, Germany) using a bilateral 2×4 array coil with two independently and freely movable 4-element coils (NORAS MRI products, Höchberg, Germany) for studies of both temporomandibular joints. Cardiac studies were performed with a 32-element receive coil combining an anterior and posterior 16-element coil. In either case, RF excitation was accomplished with the use of a circumscribing body coil.

All real-time acquisitions employed spoiled or refocused FLASH sequences as illustrated in Fig. 1 using an interleaved multi-turn radial sampling scheme and sliding window reconstructions. Although the minimum repetition time, TR, and echo time, TE, depend on experimental parameters such as the desired base resolution, which represents the number of data samples per spoke divided by the oversampling factor, these values are ultimately determined by the gradient hardware of the MRI system used. Here, the minimum TR and TE settings were exploited for real-time cardiac MRI (see below). The minimum acquisition time for a single image is given by TR $\times$ number of spokes. While it turned out to be advantageous to always exploit the minimum TR regardless of the desired imaging time (ie, spatial resolution or SNR), the choice of a suitable minimum number of spokes for acquisitions at the highest temporal resolution is limited by the chosen base resolution. This is because the gridding reconstruction only allows for moderate undersampling. For radial MRI with full data sampling the number of spokes corresponds to $\pi/2 \times$ base resolution.

Movements of the temporomandibular joint were monitored with the use of a refocused FLASH MRI sequence (Fig. 1b). Acquisitions employed a repetition time of TR = 4.33 msec, a gradient-echo time of TE = 2.10 msec, a receiver bandwidth of 810 Hz/pixel, and a flip angle of 20° for RF excitation. The images covered a 192×192 mm^2 FOV with a base resolution of 256 data samples per spoke and used 385 spokes, which roughly corresponds to a fully sampled dataset. The spokes were arranged in an interleaved 5-turn radial sampling scheme, so that image updates were reconstructed every 385/5 = 75 spokes corresponding

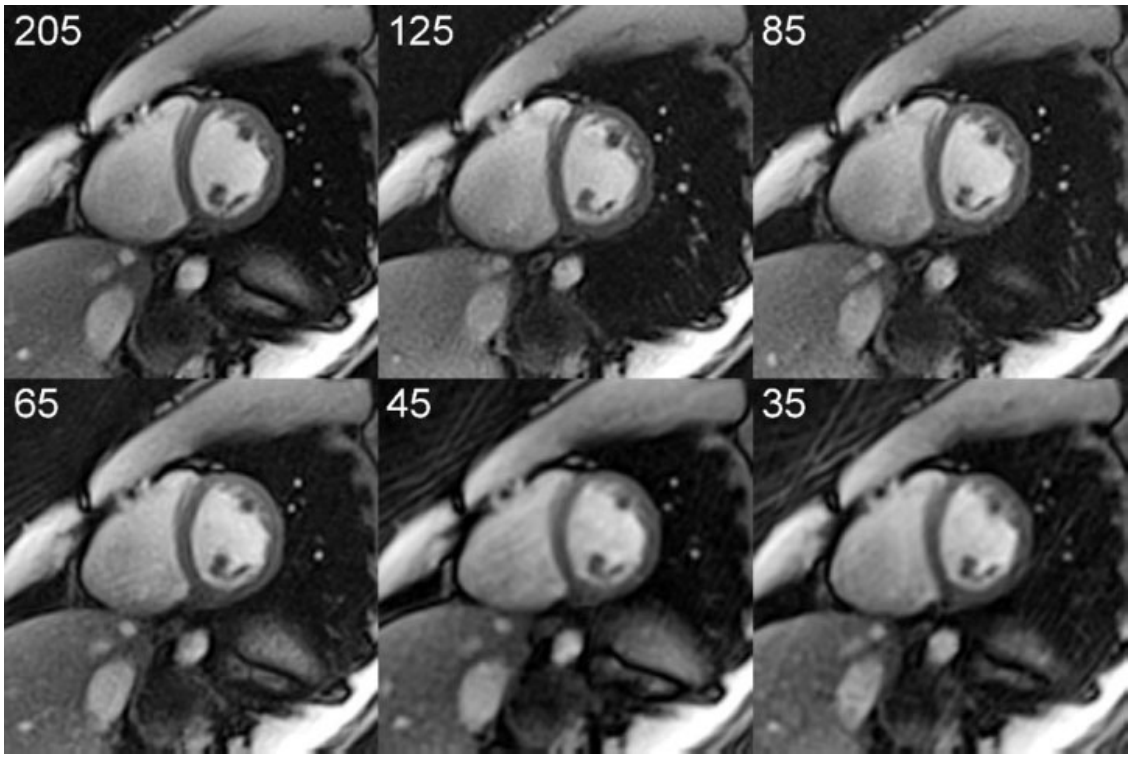

Figure 3. Undersampling of spoiled radial FLASH images of the heart (short-axis views) with a base resolution of 128 and a variable number of spokes ranging from 205 (full sampling) to 35 (TR/TE = 2.02/1.30 msec, flip angle 8°, 256 mm FOV, in-plane resolution 2 mm, slice thickness 8 mm). Choosing a number of spokes (here 125) that is similar to the base resolution ensures the absence of streaking artifacts when using conventional gridding reconstructions.

to a frame rate of 3 images per second. The in-plane resolution was 0.75 × 0.75 mm^2 with a 5-mm section thickness. Under these conditions no channel compression was necessary for real-time applications.

Cardiac real-time MRI was accomplished with the use of a spoiled FLASH MRI sequence (Fig. 1a). The repetition time was TR = 2.02 msec, the gradient-echo time TE = 1.30 msec, the receiver bandwidth 1950 Hz/pixel, and the flip angle 8°. The images covered a 256 × 256 mm^2 FOV with a base resolution of 128 data samples per spoke and used 125 spokes (moderate undersampling, see below) in an interleaved 5-turn radial sampling scheme. While the acquisition time for a single image was 250 msec, image updates were reconstructed every 25 spokes corresponding to a temporal resolution of 50 msec or a frame rate of 20 images per second. The in-plane resolution was 2 × 2 mm^2 with an 8-mm section thickness. For true real-time conditions the channel compression was set to 8 channels to avoid any detectable delay (see below).

RESULTS

Preliminary applications to healthy volunteers underline the need for a user-dependent choice of real-time MRI versions with and without refocusing of transverse coherences and confirm the preference of relatively low flip angles. This section first demonstrates some basic properties of real-time radial FLASH MRI. Subsequently, for the range of accessible experimental parameters, the selected human studies represent "extreme" examples with regard to contrast and temporal and spatial resolution.

Radial FLASH MRI

Figure 2 illustrates the motion robustness and general quality of radial FLASH images reconstructed by gridding. The images represent contiguous spoiled FLASH images from a sequential multislice acquisition that serves as a localizer tool for cardiac MRI. The acquisition time of each image was 500 msec (245 spokes, TR = 2.02 msec, TE = 1.30 msec, flip angle 8°), the in-plane resolution was 2 mm (FOV 320 mm, base resolution 160 data samples), and the slice thickness was 8 mm. Despite the relatively long acquisition time, which roughly corresponds to a fully sampled radial dataset, the images do not suffer from any ghosting artifacts due to breathing, heart motion, or vascular flow. As a consequence the availability of such multislice radial FLASH images proved to be extremely useful during the course of this study. It is foreseeable that respective sequences not only offer superior properties for a general use as localizer scans (for an arbitrary FOV), but will gain their own range of applications, for example, for rapid artifact-free abdominal imaging during free breathing.

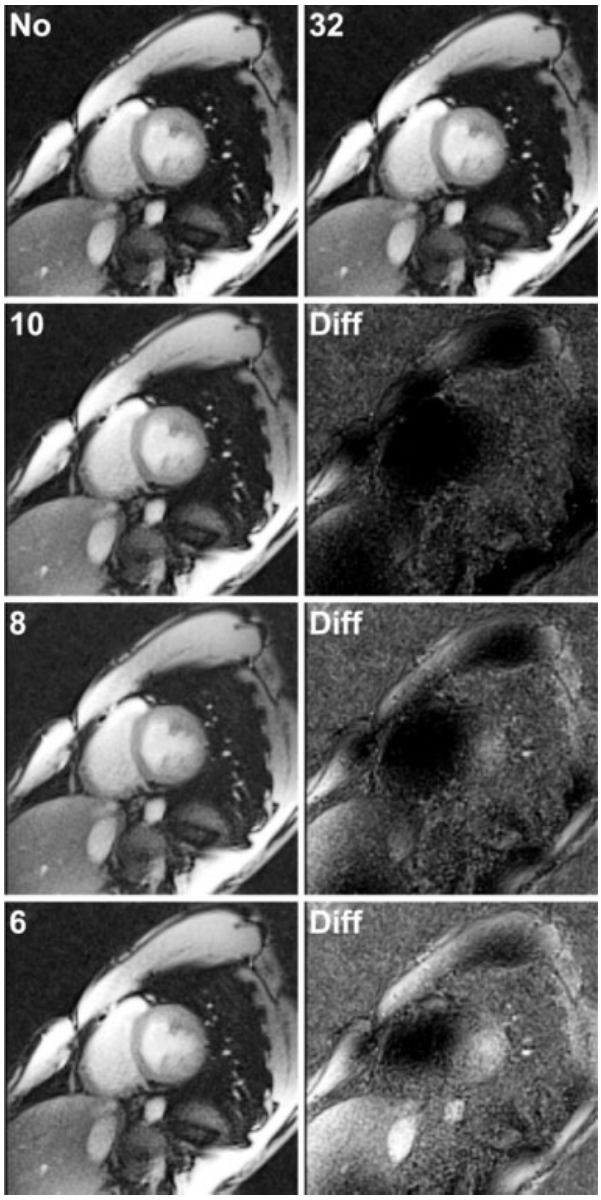

Figure 4. Channel compression for spoiled radial FLASH images of the heart (short-axis views) with an in-plane resolution of 2 mm and a slice thickness of 8 mm (TR/TE = 2.02/1.30 msec, flip angle 8°, 256 mm FOV, base resolution 128, 125 spokes). The images refer to reconstructions with (No) channel compression or the use of (32), (10), (8), and (6) eigenmodes or present (Diff) respective difference images to the 32-channel reconstruction (individual windowing to emphasize the small signals).

Figure 3 experimentally determines the ability of the gridding reconstruction to offer undistorted reconstructions for undersampled radial datasets, here for FLASH acquisitions of the heart with a base resolution of 128. The choice of a similar number of spokes as the base resolution emerged as a conservative rule of thumb that avoids visible streaking artifacts under all circumstances (here 125 spokes for a base resolution of 128). However, in many cases (depending on the actual object) the degree of undersampling might be even stronger. As shown in Fig. 3, acquisitions with only 85 spokes might have been possible. When used in combination with five interleaves and an image update after every 17 spokes (or about 34 msec), this would lead to the recording of real-time cardiac movies at about 30 frames per second.

The performance of the channel compression technique is demonstrated in Fig. 4 for the case of short-axis heart images obtained with a 32-element cardiac coil. While the images in the first row demonstrate the equivalence of the normal reconstruction from all 32 receive coils (No) with the PCA-based reconstruction from all 32 eigenmodes (32), the lower rows depict reconstructions from only 10, 8, or 6 eigenmodes as well as their respective difference images to the 32-channel reconstruction. Although the compression to a very small number of channels might introduce minor image intensity modulations or slightly lower SNR, the present choice of an 8-channel compression for cardiac studies was motivated by the need to maintain true real-time speed.

Human Studies

A first real-time application of radial FLASH MRI illustrates the continuous movement of the right temporomandibular joint during voluntary opening of the mouth in an oblique sagittal orientation, as illustrated in Fig. 5a,b. In order to ensure maximum SNR and image quality for an adequate in-plane resolution of 0.75 mm, the real-time images were obtained with a refocused radial FLASH version and full sampling. Although visible T1/T2 contrast mainly occurs within brain tissue, as shown in Fig. 5c, the signals of the joint structures were also improved in comparison to spoiled FLASH acquisitions. The serial images in Fig. 5d are magnified views selected every 5 seconds from the real-time study. They originate from a movie sequence (66 seconds duration) that covers a full cycle of slowly opening and closing the mouth at a frame rate of 3 images per second (see Supporting Movie 1). Apart from showing the anterior displacement of the condyle relative to the articular fossa, it should be noted that the articular disc remains visible during the entire movement.

An even more demanding application demonstrated in Fig. 6 is the recording of movie sequences from the heart during free breathing. The consecutive images represent spoiled radial FLASH acquisitions at the shortest possible TR and with moderate undersampling in an anatomically defined short-axis view at 2 mm in-plane resolution. Together, they correspond to a 1-second interval from a longer movie sequence (25 seconds duration) acquired at a frame rate of 20 images per second (Supporting Movie 2). The selected interval in Fig. 6 covers one cardiac cycle from end-diastole to systole and the next diastolic phase (arrows) at 50 msec temporal resolution.

DISCUSSION

The generic real-time MRI method described here offers a flexible trade-off between spatial and temporal

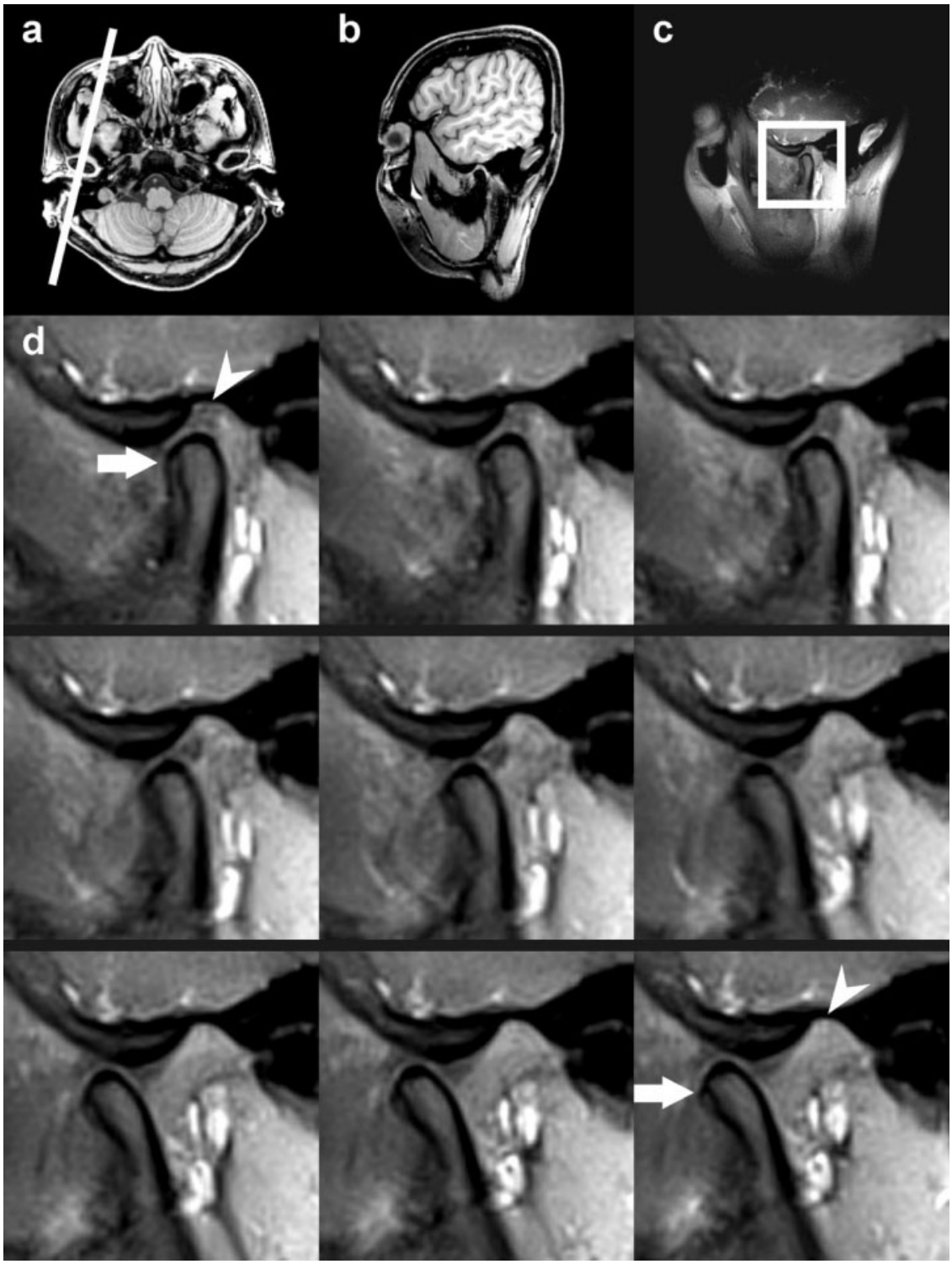

Figure 5. Real-time MRI of the temporomandibular joint during voluntary opening of the mouth at 3 Hz frame rate. **a:** Transverse and **(b)** oblique sagittal view of a healthy subject demonstrating the section for the right joint. **c:** Corresponding refocused radial FLASH image at 0.75 mm in-plane resolution and 5 mm section thickness (TR/TE = 4.33/2.10 msec, flip angle 20°, 192 mm FOV, base resolution 256, 385 spokes, image update every 75 spokes, no channel compression). **d:** Magnified views selected every 5 seconds demonstrate the anterior displacement of the condyle relative to the articular fossa (arrows).

resolution as well as T1 and T1/T2 contrast. Extending earlier work using radial FLASH MRI with refocused (13–15) or fully balanced (16–21) gradients and high flip angles, the present developments and applications to healthy human subjects demonstrate superior image quality and substantial potential for future

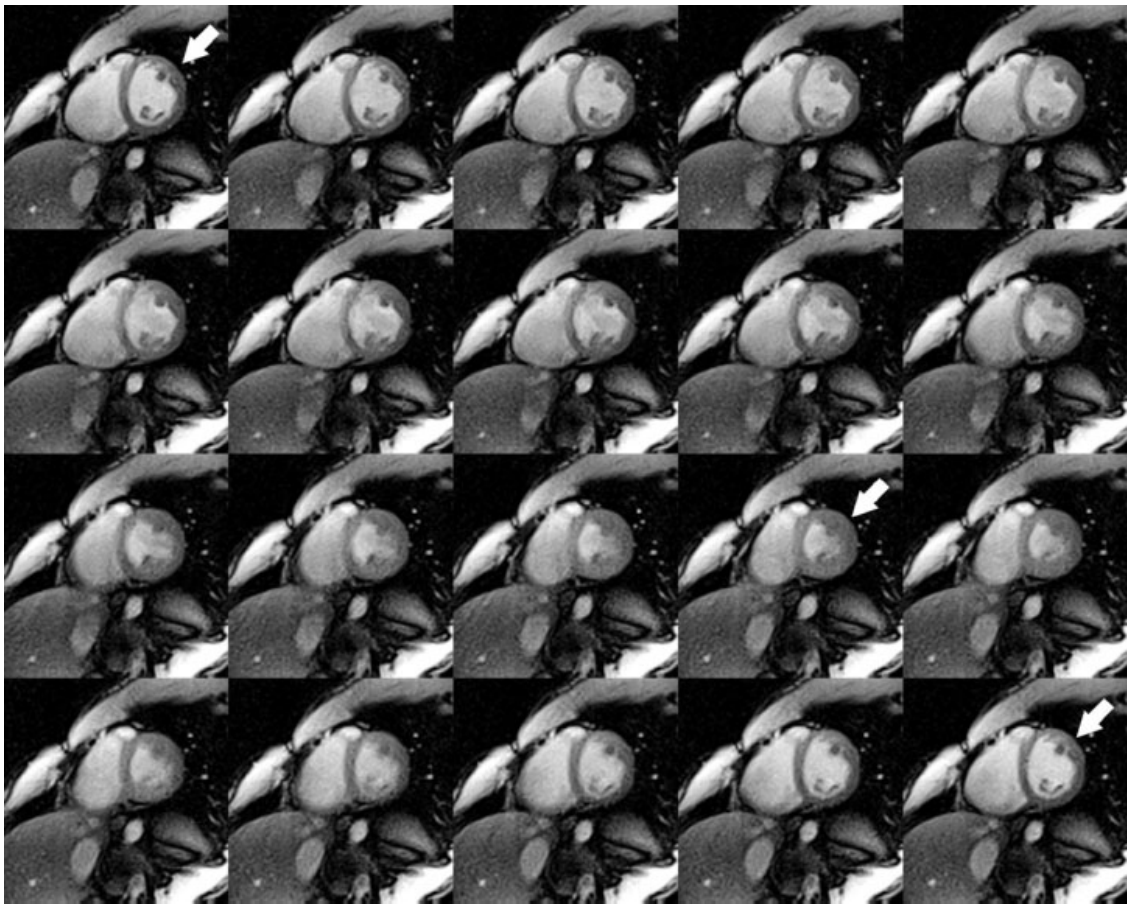

Figure 6. Real-time MRI of the heart at 20 Hz frame rate. The images (top left to lower right) were obtained from a healthy subject in a short-axis orientation using a spoiled radial FLASH sequence at 2 mm in-plane resolution and 8-mm section thickness (TR/TE = 2.02/1.30 msec, flip angle 8°, 256 mm FOV, base resolution 128, 125 spokes, image update every 25 spokes, compression to 8 channels). The image series corresponds to a 1-second period covering a full cardiac cycle from end-diastole to systole and the next diastolic phase (arrows) at 50 msec temporal resolution.

clinical applications. Nevertheless, the clinical utility of respective real-time MRI studies needs to be evaluated in much more detail and in comparison to both established MRI and non-MRI techniques such as ultrasound.

Access to T1 contrast is shown for real-time cardiac images by the occurrence of bright signals from both inflowing (unsaturated) blood and body fat (fast T1 relaxation) relative to the myocardial wall. This observation adds potential for the use of a T1-shortening contrast agent in "late enhancement" studies of patients where myocardial tissue with compromised perfusion presents with a delayed signal enhancement due to a slower or restricted uptake of the contrast agent after bolus injection.

It should also be mentioned that the proposed method reveals a negligible sensitivity to off-resonance effects as documented by the recording of head and heart images close to large air-filled spaces. This is a direct consequence of the extremely short echo times of 1–2 msec used here. It also promises artifact-free visualizations of surgical instruments in the imaging FOV.

Another aspect of real-time MRI is the achievable temporal resolution and the amount of residual temporal blurring. In this context it is fair to acknowledge that the true image acquisition time without sliding window reconstruction determines the basic temporal fidelity as defined by the sharpness or accuracy of the individual images. On the other hand, because the spokes of a radial acquisition overlap in the center of *k*-space, a sliding window reconstruction of serial datasets benefits from an update of low spatial frequencies with each acquired spoke, which continuously adds new motion-related information to the images. In the future the application of recently developed iterative reconstruction algorithms for strongly undersampled radial MRI data (10,27) is expected to further enhance the true temporal resolution. This is due to the fact that such methods allow for a much higher degree of radial undersampling than a gridding reconstruction as used here, which directly translates into shorter image acquisition times. At this stage, however, the high computational requirement of these techniques prevents their use for real-time applications.

In conclusion, real-time radial FLASH MRI emerges as a simple and robust method that is easily implementable on existing MRI systems. The physical

properties demonstrated here render it most suitable for studies of joint movements and cardiac functions as well as for imaging of the liver and gastrointestinal tract, for fetal imaging, and for dynamic perfusion studies that monitor the uptake and clearance of a contrast agent. Moreover, the method will largely facilitate MRI-guided interventions ranging from the control of biopsies to minimally invasive procedures such as the placement of an endovascular stent graft.

ACKNOWLEDGMENT

The authors thank Dirk Voit and Klaus-Dietmar Merboldt for help in sequence development and Peter Dechent for loaning the 32-element cardiac coil.

REFERENCES

1. Lauterbur PC. Image formation by induced local interactions: examples employing nuclear magnetic resonance. Nature 1973; 242:190–191.
2. Frahm J, Haase A, Matthaei D. Rapid NMR imaging of dynamic processes using the FLASH technique. Magn Reson Med 1986;3: 321–327.
3. Riederer SJ, Tasciyan T, Farzaneh F, Lee JN, Wright RC, Herfkens RJ. MR fluoroscopy: technical feasibility. Magn Reson Med 1988;8:1–15.
4. Kerr AB, Pauly JM, Hu BS, et al. Real-time interactive MRI on a conventional scanner. Magn Reson Med 1997;38:355–367.
5. Nayak KS, Pauly JM, Yang PC, Hu BS, Meyer CH, Nishimura DG. Real-time interactive coronary MRA. Magn Reson Med 2001;46: 430–435.
6. Narayanan S, Nayak K, Byrd D, Lee S. An approach to real-time magnetic resonance imaging for speech production. J Acoust Soc Am 2004;115:1771–1776.
7. Draper CE, Santos JM, Kourtis LC, et al. Feasibility of using real-time MRI to measure joint kinematics in 1.5 T and open-bore 0.5 T systems. J Magn Reson Imaging 2008;28:158–166.
8. Scheffler K, Hennig J. Reduced circular field-of-view imaging. Magn Reson Med 1998;40:474–480.
9. Peters DC, Korosec FR, Grist TM, et al. Undersampled projection reconstruction applied to MR angiography. Magn Reson Med 2000;43:91–101.
10. Block TK, Uecker M, Frahm J. Undersampled radial MRI with multiple coils. Iterative image reconstruction using a total variation constraint. Magn Reson Med 2007;57:1086–1098.
11. Speier P, Trautwein F. Robust radial imaging with predetermined isotropic gradient delay correction. In: Proc 14th Annual Meeting ISMRM, Seattle; 2006: 2379.
12. Debbins JP, Riederer SJ, Rossman PJ, et al. Cardiac magnetic resonance fluoroscopy. Magn Reson Med 1996;36:588–595.
13. Rasche V, de Boer RW, Holz D, Proksa R. Continuous radial data acquisition for dynamic MRI. Magn Reson Med 1995;34:754–761.
14. Rasche V, Holz D, Köhler J, Proksa R, Roeschmann P. Catheter tracking using continuous radial MRI. Magn Reson Med 1997;37: 963–968.
15. Rasche V, Holz D, Proksa R. MR fluoroscopy using projection reconstruction multi-gradient-echo (prMGE) MRI. Magn Reson Med 1999;42:324–334.
16. Shankaranarayanan A, Simonetti OP, Laub G, Lewin JS, Duerk JL. Segmented k-space and real-time cardiac cine MR imaging with radial trajectories. Radiology 2001;221:827–836.
17. Spuentrup E, Ruebben A, Schaeffter T, Manning WJ, Günther RW, Buecker A. Magnetic resonance-guided coronary artery stent placement in a swine model. Circulation 2002;105:874–879.
18. Peters DC, Lederman RJ, Dick AJ, et al. Undersampled projection reconstruction for active catheter imaging with adaptable temporal resolution and catheter-only views. Magn Reson Med 2003; 49:216–222.
19. McLeish K, Kozerke S, Crum WR, Hill DLG. Free-breathing radial acquisitions of the heart. Magn Reson Med 2004;52:1127–1135.
20. Eggebrecht H, Kühl H, Kaiser GM, et al. Feasibility of real-time magnetic resonance-guided stent-graft placement in a swine model of descending aortic dissection. Eur Heart J 2006;27: 613–620.
21. Leung AO, Paterson I, Thompson RB. Free-breathing cine MRI. Magn Reson Med 2008;60:1709–717.
22. O'Sullivan JD. A fast sinc function gridding algorithm for Fourier inversion in computer tomography. IEEE Trans Med Imaging 1985;4:200–207.
23. Kaiser JF. Nonrecursive digital filter design using the I_0-SINH window function. In: Proc IEEE Int Symp Circuits Syst 1974; 20–23.
24. Jackson JI, Meyer CG, Nishimura DG. Selection of a convolution function for Fourier inversion using gridding. IEEE Trans Med Imaging 1991;10:473–478.
25. Huang F, Vijayakumar S, Li Y, Hertel S, Duensing GR. A software channel compression technique for faster reconstruction with many channels. Magn Reson Imaging 2008;26:133–141.
26. Buehrer M, Pruessmann KP, Boesiger P, Kozerke S. Array compression for MRI with large coil arrays. Magn Reson Med 2007; 57:1131–1139.
27. Gamper U, Boesiger P, Kozerke S. Compressed sensing in dynamic MRI. Magn Reson Med 2008;59:365–373.